

# Interferometry using Phase Slope Estimation

Stig A V Synnes<sup>1,2</sup>, Torstein O Sæbø<sup>1</sup>, Roy E Hansen<sup>1,2</sup>

1) Norwegian Defence Research Establishment (FFI), PO Box 25, NO-2027 Kjeller, Norway

2) University of Oslo (UiO), Department of Informatics, PO Box 1080, Blindern, N-0316 Oslo, Norway

## Abstract

The terrain elevation can be estimated with active radar and sonar by observing the scene from vertically displaced sensors and estimating the difference in time of arrival of the signal returns. A high precision estimate is available from the phase difference between preregistered time series. This estimate has an inherent  $2\pi$  wrap ambiguity, but the dynamics over the signal bandwidth can be used to estimate the correct wrap. Common absolute phase estimators based on either cross-correlation or the phase slope between sub-band images, depend on either spatial smoothing or down-sampling. We propose a generalization of the sub-band methods for phase slope estimation that has the potential of providing absolute phase estimates at full image resolution.

## 1 Introduction

The terrain elevation can be estimated using radar and sonar by observing the scene from vertically displaced sensors. An interferogram can be formed to retrieve the phase difference between the matched filtered time series at two receivers. The interferometric phase estimate has an inherent  $2\pi$  wrap ambiguity, and additional information is needed in order to obtain the absolute phase.

One approach of estimating the absolute phase based on broadband information is to search for the maximum amplitude of a sliding window cross-correlation [1]. Another approach is to estimate the phase slope between sub-band images, as with Delta-k / split-spectrum algorithm (SSA) [2, 3] or the multi-chromatic approach (MCA) [4, 5]. The performance of different methods have been compared in [6]. We note that some degree of spatial smoothing or down-sampling is inherent to all of these established methods.

We propose a method for phase slope estimation that has the potential of providing absolute phase estimates at full image resolution. The core steps are to create a frequency domain representation of the full time series, spatially focus it onto each pixel, and estimate the phase slope at the pixel. We present the method as a generalization of the sub-band approach.

The phase slope represents the time delay and is independent of frequency. It is estimated in the frequency domain, but since no frequency resolution is acquired, there is no inherent spatial averaging. Therefore independent estimates should be available at full spatial resolution.

In Section 2 we outline the measurement geometry and the signal model, along with the fundamentals of both interferometry and phase slope estimation. In Section 3 we develop the method from the sub-band method of absolute phase slope estimation. We finally present results on simulated data for a system with 30% relative bandwidth in Section 4, before we conclude in Section 5.

## 2 Estimation of Terrain Elevation

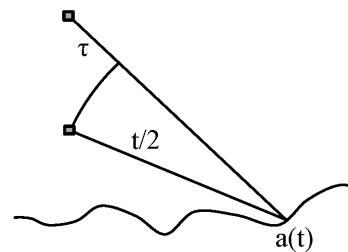


**Figure 1:** Geometry for estimation of terrain elevation using interferometric measurements. The ground reflectivity function  $a(t)$  is recorded from two vertically displaced receivers. In this illustration we have assumed that the transmitter is co-located with the lower receiver.

We assume a measurement geometry as in Figure 1, and consider the location observed by the lower sensor at time  $t$ . The elevation at this location can be estimated from the time delay  $\tau$  at which the same location is observed by the upper sensor. We adopt a signal model with a complex reflectivity coefficient  $a(t, \omega)$ , for time  $t$  and angular frequency  $\omega$ . We denote the lower receiver "primary",  $p$ , and the upper receiver "secondary",  $s$ , and obtain

$$p(t, \omega) = a(t, \omega)e^{-i\omega t} \quad (1)$$

$$s(t + \tau(t), \omega) = a(t, \omega)e^{-i\omega(t + \tau(t))} \quad (2)$$

where we have assumed that  $t + \tau(t)$  is monotonically increasing. This corresponds to a terrain elevation profile that does not cause layover, shadow or multiple scattering. Then  $s(t + \tau(t))$  is locally a time-shifted replica of  $p(t)$ , and we obtain

$$\psi(t, \tau(t), \omega) = s^*(t + \tau(t), \omega)p(t, \omega) \quad (3)$$

$$= |a(t, \omega)|^2 e^{i\omega\tau(t)}. \quad (4)$$

With co-registered reflectivity functions, the absolute phase shift  $\varphi_a$  is a function of frequency and time delay,

$$\varphi_a(\tau, \omega) = \omega\tau. \quad (5)$$

Equations (3)-(4) give the interferogram for the co-registered reflectivity functions. The angle of the interferogram,  $\angle\psi$ , provides the absolute phase  $\varphi_a$  modulus  $2\pi$ .

By differentiating the absolute phase of equation (5) with respect to the angular frequency, we obtain the phase slope, which provides a frequency-independent estimate of the time delay,

$$\tau = \frac{\delta\varphi_a(\omega, \tau)}{\delta\omega}. \quad (6)$$

### 3 Full Band Phase Slope Estimation

An interferogram can be made at image resolution, making use of the full signal bandwidth. In contrast, the sub-band approach forms interferograms on each subband, giving lower resolution interferograms. These are subsequently used for estimating the phase slope. Thus, while the full band interferogram take advantage of all the information (and meets the Cramér-Rao Lower Bound at the correct time delay), the subband approach do not take full advantage of the data, as it operates on down-sampled data only. We present a generalization of the subband approach that does not rely on down-sampling the data.

From equation (6) we know that the phase slope should be consistent over all frequencies, and thus the contributions from all frequencies could be combined to provide the same spatial resolution as for image amplitude variations.

In order to estimate the contribution to the phase slope estimates from each frequency, we decompose the signal into its individual frequency components and focus these onto the pixel under investigation. This operation is presented in Section 3.1. Next we expand the interferogram through a frequential cross-correlation matrix in Section 3.2, before we express the sub-band method through a sub-set of the same matrix elements in Section 3.3. We finally suggest an approach for estimating the phase slope at each time sample in Section 3.4.

#### 3.1 Fixed-Time Frequency-Decomposition

Here we compute the frequency domain spectrum, focused onto a time sample of choice. This is obtained by first applying the Fourier transform, before preparing the terms of the inverse Fourier transform, but without adding the terms together. This approach was inspired by [7], and is detailed below.

We first compute the Fourier coefficients for the primary time series, where we use  $n_t \in [0, N - 1]$  as index for the time samples and  $n_\omega \in [0, N - 1]$  as index for the frequency samples:

$$P[n_\omega] = \sum_{n_t \in [0, N-1]} p[n_t] e^{-in_\omega n_t / N} \quad (7)$$

We then express the time samples by use of the inverse Fourier transform:

$$p[n_t] = \sum_{n_\omega \in [0, N-1]} P[n_\omega] e^{in_\omega n_t / N} \quad (8)$$

We do not sum at this point, but rather collect the terms within the summation. These can be expressed recursively for different time samples:

$$\begin{aligned} Q[n_t, n_\omega] &= P[n_\omega] e^{in_\omega n_t / N} \quad (9) \\ &= Q[n_{t_0}, n_\omega] \cdot e^{in_\omega (n_t - n_{t_0}) / N} \quad (10) \end{aligned}$$

#### 3.2 Full Band Interferogram

For familiarity, we first rewrite the zero-lag interferogram at full resolution (using all samples or the full bandwidth). With the zero-lag interferogram we here mean without any shift applied to compensate for the time delay:

$$\psi(n_t) = p^*(n_t) s(n_t) \quad (11)$$

Next we rewrite the interferogram in terms of the fixed-time frequency components of the primary signal  $Q$  and secondary signal  $R$ :

$$\psi(n_t) = \sum_{n_\omega \in [0, N-1]} Q^*[n_t, n_\omega] \sum_{m_\omega \in [0, N-1]} R[n_t, m_\omega] \quad (12)$$

This equation can be written out in matrix form. In order to simplify the matrix, we define  $Q_m = Q[n_t, m - 1]$  and  $R_m = R[n_t, m - 1]$  and obtain for any time sample  $n_t$ :

$$\psi = \sum \begin{bmatrix} Q_1^* R_1 & Q_1^* R_2 & \dots & Q_1^* R_N \\ Q_2^* R_1 & Q_2^* R_2 & \dots & Q_2^* R_N \\ \vdots & \vdots & \ddots & \vdots \\ Q_N^* R_1 & Q_N^* R_2 & \dots & Q_N^* R_N \end{bmatrix} \quad (13)$$

where we let  $\sum [\cdot]$  denote the sum over all the matrix elements. The matrix of equation (13) can be interpreted as a frequential cross-correlation matrix.

#### 3.3 Subband Interferograms

We now study how the subband approach addresses the elements of the frequential cross-correlation matrix of equation (13). We let  $\psi_{c/C}$  denote the subband interferograms for band  $c$  out of totally  $C$  non-overlapping bands that together span the full bandwidth.

The full band interferogram,  $\psi_{1/1}$  of equation (13) is rewritten in equation (14), but here we also indicate the sub-matrices used to compute each of the three subband interferograms  $\psi_{1/3}$ ,  $\psi_{2/3}$  and  $\psi_{3/3}$ .

$$\psi_{1/1} = \sum \begin{bmatrix} [\psi_{1/3}] & \dots \\ \vdots & [\psi_{2/3}] & \vdots \\ \dots & \dots & [\psi_{3/3}] \end{bmatrix} \quad (14)$$

### 3.4 Full Band Phase Slope

We note that although the subband interferograms of equation (14) together span the full bandwidth, they only use a fraction  $1/C$  of the matrix elements used by the full bandwidth interferogram. Decreasing the subband width degraded the resolution correspondingly.

We note that the frequency related to each matrix element increases along the diagonal from the upper left corner to the lower right corner of the frequential cross-correlation matrix. We now assume that the off-diagonal position represent different pixel shifts of the time series. We postulate that the frequency-dependent phase slope for any shift can be obtained by summing all of the elements orthogonal to the diagonal. We can then form a vector of phase slope measurements by applying the sum over all elements along the axis orthogonal to the diagonal and obtain a vector of elements  $D_a$ .

$$D_a = \sum_{\forall n,m(n+m)/2=a} Q_n^* R_m \quad (15)$$

The elements  $D_a$  of the vector relates to measurements at angular frequencies  $\omega_a$  for the combination of  $\omega_n$  and  $\omega_m$  for any/all  $Q_n^* R_m$  going into  $D_a$ :

$$\omega_a = (\omega_n + \omega_m)/2 \quad (16)$$

We let  $D$  and  $W$  denote the vector of elements  $D_a$  and  $\omega_a$  correspondingly.

With equation (6) we established that the phase slope is identical to the time delay. The time delay is independent of frequency, and we thus have  $2N - 1$  estimates of it. In order to obtain the best possible estimate of the time delay  $\tau_n$  for time  $t_n$  at the primary array, all estimates must be employed and weighted in accordance with their contribution of the frequency component into the pixel. We construct a model describing the frequency-dependent phasor  $M$  that is a solution to equation (6):

$$M(\omega) = e^{i\omega\tau} \quad (17)$$

The component of  $D$  that is in phase with  $M$  follows as:

$$A(\tau) = \sum_{\omega} D(\omega) M^*(\tau, \omega) \quad (18)$$

A best fit solution can be approached by searching for the time delay  $\tau$  that minimizes the error between the model and the measurement in a least squares sense, using the signal amplitude  $|M|$  as weights. Equation (18) gives the phase corrected interferogram [8, p 98].

## 4 Results and Discussion

For now we search for the time delay  $\tau$  that maximizes  $A(\tau)$ , i.e. the signal aligned with the modelled phase slope, and we ignore the orthogonal component. The signal amplitude has been used for weighting the contributions from each frequency. The default Matlab2014b `fminsearch` algorithm has been applied on  $-|A(\tau)|$  with

custom termination limits. The search was started near  $\tau = 0$ , and we let the first local maximum provide our estimate of the phase slope. The estimate is in general more accurate than that of a zero-lag assumption, but its precision is low compared to that of the interferogram. We therefore shift the time series in accordance with the phase slope and refine the time delay estimate by use of the residual phase, as for the interferogram.

We present results for the method on simulated data for a HISAS synthetic aperture sonar operated on the HUGIN autonomous underwater vehicle [6]. The sensor is a 100 kHz sonar (1.5 cm wavelength) with 30% relative bandwidth and 30 cm receiver spacing. The simulated scene spans 200 m and is observed from an elevation of 15 m. It contains a speckle scene of a flat bottom geometry with three rectangular boxes and one triangular box. In Figure 2 we present results on the simulated scene as absolute phase delays.

The phase slope results (without refinement) are presented in the left panels. We observe that the time delays based on phase slope estimation has a tight distribution around the true elevation of the scene, but we also observe a lot of outliers. The distribution is broadened with the introduction of additive noise, i.e. from the upper panels to the lower panels. Any noise contribution on the upper panels is believed to come from range-sidelobes from nearby reflectors. Our investigations indicate that the time delays around the true solution correspond to solutions on the correct local maximum, while the outliers correspond to detection on other local maxima. Around the rapidly changing height variations at the edges of the boxes, even the true solution looks noisy. This is a result of analytically combining the layover data for the assumption of only one elevation.

The phase slope results with refinement by the residual phase are presented in the right panels. As expected, this step focuses the distribution of the absolute phase estimates within the already assigned wrap.

Future work could include a metric of quality, with application such as rating the valid estimates and identifying outliers. Also a method for combining nearby estimates into a more robust estimate should be considered.

## 5 Conclusion

We have presented a method for phase slope estimation that has the potential of providing absolute phase estimates at image resolution. The method has been presented as a generalization of the sub-band approach. We have applied the method on a simulated speckle scene without and with noise, and have shown that the majority of the time delay estimates are distributed around the true solution. However, a large number of outliers are also present, and these are probably related to the search algorithm picking the wrong local maximum.

Further investigations should include a performance metric. Though the time delay estimates are provided at full image resolution, it remains to determine the quality of

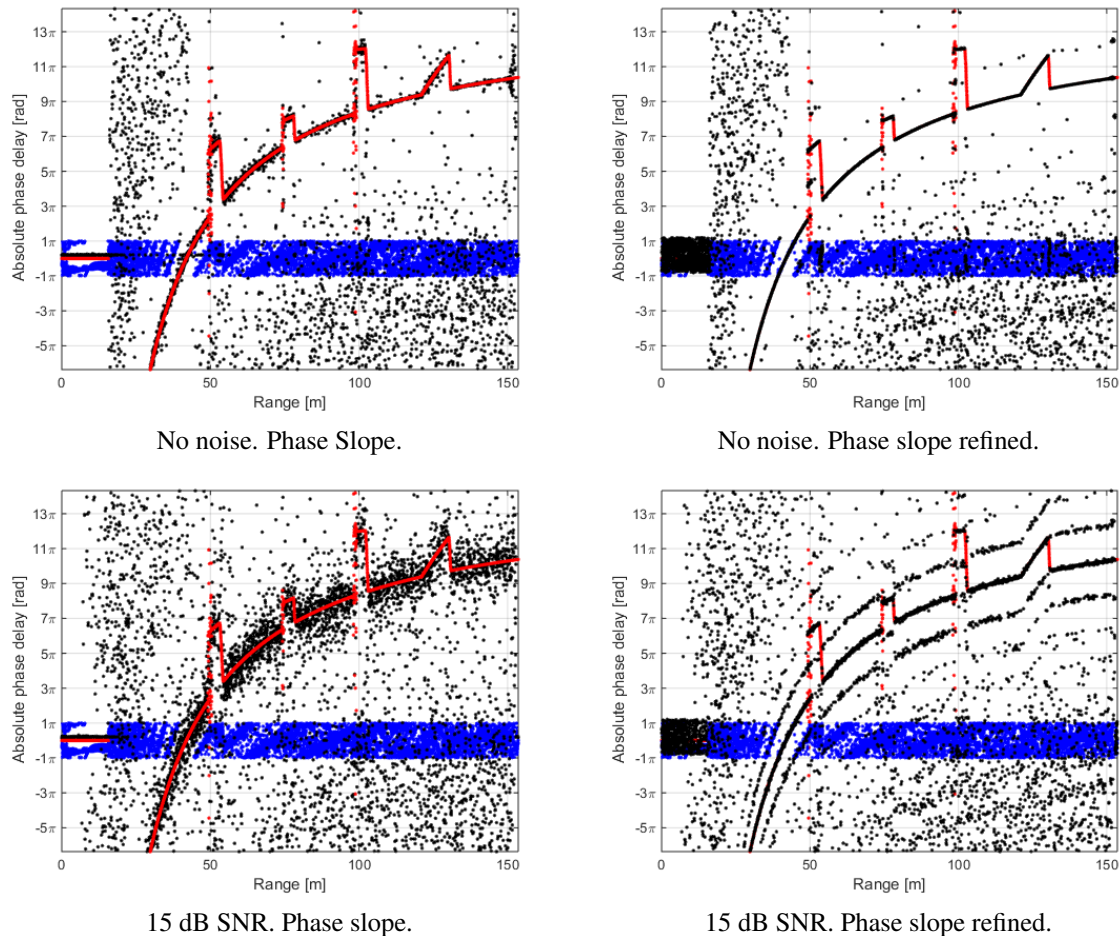


**Figure 2:** Time delay estimates for simulated data from a speckle scene with three rectangular boxes and one triangular box on an otherwise flat seafloor, observed at 15 m altitude by a system of 30% relative bandwidth. The true solution is presented in red, the interferogram in blue, and the phase slope estimates in black. The top row is for a simulation without noise, and the bottom row is for 15 dB SNR. The left column results are for phase slope estimates only and right column results are for phase slope estimates refined by the residual phase.

these estimates. It also remains to investigate the independency of neighbour estimates (the resolution) and how to best combine measurements over an interval to provide a given accuracy.

## References

- [1] S. N. Madsen. Absolute phase determination techniques in SAR interferometry. In *Proceedings of SPIE*, volume 2487, Orlando, United States, 1995.
- [2] R. Bamler and M. Eineder. Accuracy of differential shift estimation by correlation and split-bandwidth interferometry for wideband and delta-k SAR systems. *IEEE Geosci. Remote Sens. Lett.*, 2(2):151–155, 2005.
- [3] S. N. Madsen and H. A. Zebker. Automated absolute phase retrieval in across-track interferometry. In *Proceedings of IGARSS'92*, pages 1582–1584, Houston, Texas, 1992.
- [4] N. Veneziani, F. Bovenga, and A. Refice. A wide-band approach to the absolute phase retrieval in SAR interferometry. *Multidimensional Systems and Signal Processing*, 14:183–205, 2003.
- [5] F. Bovenga, V. M. Giacobozzo, A. Refice, and N. Veneziani. Multichromatic analysis of InSAR data. *IEEE Transactions on Geoscience and Remote Sensing*, 51(9):4790–4799, 2013.
- [6] T. O. Sæbø, S. A. V. Synnes, and R. E. Hansen. Wide-band Interferometry in Synthetic Aperture Sonar. *IEEE Trans. Geosci. Remote Sens.*, 51(8):4450–4459, 2013.
- [7] S. A. V. Synnes and R. E. Hansen. Aspect-dependent scattering in widebeam synthetic aperture sonar. In *UACE 2015*, Crete, Greece, 2015.
- [8] R. F. Hanssen. *Radar Interferometry: Data Interpretation and Error Analysis*. Kluwer Academic Publishers, Dordrecht, The Netherlands, 2001.